

**High-pressure synthesis, characterization, and equation of state of cubic C-BN solid solutions**

E. Knittle\*

*Department of Earth Sciences and Institute of Tectonics, University of California, Santa Cruz, California 95064*

R. B. Kaner

*Department of Chemistry and Biochemistry, University of California, Los Angeles, California 90024*

R. Jeanloz

*Department of Geology and Geophysics, University of California, Berkeley, California 94720*

M. L. Cohen

*Department of Physics, University of California, Berkeley and Materials Science Division, Lawrence Berkeley Laboratory, Berkeley, California 94720*

(Received 2 August 1994)

Synthesis of several samples across the cubic  $C_x(BN)_{1-x}$  solid solution ( $x=0.3-0.33, 0.5, 0.6$ ) at pressures in excess of 30 GPa and temperatures above 1500 K indicates that they are isostructural with diamond and cubic BN (borazon). Measurement of the lattice parameters of C-BN samples quenched to ambient conditions shows that the solid solution between C (diamond) and cubic BN is nonideal, with unit-cell volumes up to 1% larger than predicted based on ideal mixing (Vegard's law). In addition, we have measured the zero-pressure, 300-K vibrational spectra for  $C_{0.3}(BN)_{0.7}$ . In the midinfrared absorption spectrum, we observe a reststrahlen band ranging from 1000–1120  $\text{cm}^{-1}$ , and the Raman spectrum has a longitudinal optic mode at 1323( $\pm 2$ )  $\text{cm}^{-1}$ . Based on a comparison of the spectrum with that of diamond and cubic-BN, we conclude that the bonding in cubic C-BN is partially ionic. In addition to these measurements on quenched samples, we have measured the isothermal bulk modulus of  $C_{0.33}(BN)_{0.67}$  by x-ray diffraction through a diamond cell to over 100 GPa at 300 K. The bulk modulus is 355( $\pm 19$ ) GPa, which is lower than those of diamond, cubic BN and the value predicted from ideal mixing between the end members, but is consistent with the nonideal expansion observed for the cubic C-BN lattice parameters.

**INTRODUCTION**

The cubic, high-pressure-temperature polymorphs of carbon (diamond) and boron nitride (borazon) are the hardest of all known solids. They share a number of similar physical properties including high melting temperatures ( $> 3000$  K), large bulk moduli (442 and 369 GPa for C and BN, respectively), high thermal conductivities ( $\sim 200 \text{ W m}^{-1} \text{ K}^{-1}$ ) and chemical inertness.<sup>1-3</sup> In addition, the phase diagrams of both C and BN are similar, including a hexagonal-graphitic structure as their stable form at ambient conditions, and a high-pressure-temperature hexagonal (würtzite) structure as well as the diamondlike (cubic) form.<sup>4-14</sup> Given the similarity in their phase diagrams and their atomic sizes, it is anticipated that a solid solution should exist across the carbon-boron nitride system at high pressure. Indeed, there is a report in the literature of one such compound being synthesized.<sup>15</sup> Such solid solutions may have physical properties similar to diamond and borazon, and are therefore of potential technological importance.

Here we report the synthesis of several cubic (zinc-blende-structured) C-BN solid solutions using the laser-heated diamond cell. We have examined the samples quenched from high pressures and temperatures (which, as with diamond and borazon, are metastable at ambient

conditions) using x-ray diffraction and, where possible, Raman and transmission infrared spectroscopy at 300 K. Thus, we have measured the effect of composition on the lattice parameters and vibrational frequencies of samples across the C-BN solid solution. In addition, using x-ray diffraction at high pressures and 300 K, we have measured the isothermal bulk modulus of  $C_x(BN)_{1-x}$  ( $x \sim 0.33$ ) for comparison with the values for diamond and borazon.

**EXPERIMENTAL**

To examine the dependence of lattice parameter on composition for cubic (zinc-blende) structured C-BN, we used two different types of starting materials. The first were microcrystalline C-BN compounds with approximate stoichiometries of  $C_{0.3}(BN)_{0.7}$  and  $C_{0.6}(BN)_{0.4}$  based on carbon chemical analysis.<sup>16</sup> The second-type of starting material were three different mechanical mixtures of graphite-structured BN (*g*-BN) and C (*g*-C) with stoichiometries of  $C_{0.33}(BN)_{0.66}$ ,  $C_{0.5}(BN)_{0.5}$ , and  $C_{0.6}(BN)_{0.4}$ . The first composition,  $C_{0.33}(BN)_{0.67}$ , represents  $C_xB_xN_x$  where  $x \sim 0.33$  and is used for comparison with the synthetic, microcrystalline  $C_{0.3}(BN)_{0.7}$  composition. The graphite-structured powders were ground together under acetone to powders of  $\sim 1 \mu\text{m}$

TABLE I. X-ray-diffraction results: zero pressure, 300 K.

Composition <sup>a</sup>	<i>d</i> spacing (Å) <sup>b</sup>	<i>hkl</i>
Cubic-BN	1.090±0.004 ( <i>w</i> )	311
	1.279±0.003 ( <i>m</i> )	220
	1.809±0.005 ( <i>w</i> )	200
	2.089±0.003 ( <i>vs</i> )	111
C <sub>0.3</sub> (BN) <sub>0.7</sub> ( <i>m</i> )	1.276±0.005 ( <i>w</i> )	220
	1.806±0.005 ( <i>vw</i> )	200
	2.086±0.002 ( <i>s</i> )	111
C <sub>0.33</sub> (BN) <sub>0.67</sub> ( <i>g</i> )	1.278±0.007 ( <i>w</i> )	220
	2.086±0.001 ( <i>s</i> )	111
C <sub>0.5</sub> (BN) <sub>0.5</sub> ( <i>g</i> )	1.270±0.005 ( <i>w</i> )	220
	2.080±0.002 ( <i>s</i> )	111
C <sub>0.6</sub> (BN) <sub>0.4</sub> ( <i>m</i> )	1.269±0.006 ( <i>w</i> )	220
	1.798±0.008 ( <i>vw</i> )	200
	2.075±0.005 ( <i>s</i> )	111
C <sub>0.6</sub> (BN) <sub>0.4</sub> ( <i>g</i> )	1.267±0.006 ( <i>w</i> )	220
	2.076±0.003 ( <i>s</i> )	111

<sup>a</sup>The starting material is given in parentheses after the composition: (*m*) indicates microcrystalline starting material, (*g*) indicates a mechanical mixture of graphitic carbon and boron nitride.

<sup>b</sup>Intensities are estimated visually: *vw*=very weak, *w*=weak, *m*=medium, *s*=strong, *vs*=very strong.

grain size.

A Mao-Bell-type diamond cell was used to compress the samples in a gasketed configuration, with pressure determined using the standard ruby fluorescence method.<sup>17</sup> After compression, the samples were heated for 5–10 min with a Nd:YAG laser (with an output of 25 W at 1064 nm in TEM<sub>00</sub> mode) focused into the sample through a microscope.<sup>18</sup> Average temperatures in the laser-heated spots were measured using a spectroradiometric technique.<sup>18,19</sup> Typical synthesis conditions for the cubic, high *P-T* phases were pressures of 30–50 GPa

and temperatures between 2000 and 2500 K (±200–250 K; see also Tables I and II for specifics of the synthesis conditions of each experiment). Because of the small grain size of the samples, the high-pressure phases appeared opaque after heating when observed *in situ* through the diamond cell.

After conversion to the high-pressure phase, the samples were quenched in pressure and temperature and removed from the diamond cell for phase identification using x-ray diffraction. Samples were loaded into a 114.6 mm Debye-Scherrer camera and x-ray patterns were collected on film using Cu *K*α radiation. For comparison with our cubic C-BN samples, we also remeasured the zero-pressure x-ray patterns of cubic-BN (supplied by R. C. DeVries, see also Ref. 3) and diamond in the same experimental configuration we used for the newly synthesized cubic phases.

Raman spectra of two of the quenched C<sub>0.3</sub>(BN)<sub>0.7</sub> samples synthesized from the microcrystalline starting material at 30 and 50 GPa were also measured. The samples were crushed to obtain transparent flakes. An 18 mW He-Ne laser at 632.8 nm (plasma lines removed using an Optometrics tunable grating filter) was focused into the sample through an Olympus microscope to excite the Raman effect. The scattered light was collected in a ~360° scattering geometry and focused into a SPEX Triplemate spectrograph. The spectra were recorded with an imaging multichannel plate detector with a resolution of 2 cm<sup>-1</sup>. Spectra of diamond and cubic BN were also measured in the same experimental configuration to compare with the spectrum of cubic C-BN.

As a complement to the Raman spectra, we also obtained zero-pressure transmission infrared spectrum of the quenched samples synthesized at 30 GPa. Three samples [~0.1 mg of C<sub>0.3</sub>(BN)<sub>0.7</sub>] were ground in ~1 mg of spectroscopic-grade KBr and pressed into a 1 mm diameter pellet. The spectra were measured using a DigiLab FTS-80 Fourier-transform infrared spectrometer

TABLE II. Lattice parameters for cubic C-BN solid solutions.

Composition	Synthesis pressure (GPa) <sup>a</sup>	Lattice parameter (Å)	<i>hkl</i>	References
C (diamond)		3.567±0.001	111,200, 220,311	This study JCPDS No. 6-0675
BN (borazon)		3.617±0.001	111,200, 220,311	This study JCPDS No. 35-1365
C <sub>0.6</sub> (BN) <sub>0.4</sub>	30±5 <sup>b</sup> , 40±7 <sup>c</sup>	3.596±0.003	111,200,220	This study <sup>d</sup>
C <sub>0.5</sub> (BN) <sub>0.5</sub>	35±4 <sup>b</sup>	3.602±0.003	111,220	This study <sup>e</sup>
C <sub>0.3-0.33</sub> (BN) <sub>0.67-0.7</sub>	30±3 <sup>b,c</sup> , 50±10 <sup>c</sup>	3.613±0.003	111,200,220	This study <sup>d</sup>

<sup>a</sup>Pressure is measured using the ruby fluorescence technique.

<sup>b</sup>Synthesis pressure of cubic C-BN made from a mechanical mixture of graphite-structured C and BN.

<sup>c</sup>Synthesis pressure of cubic C-BN made from microcrystalline C-BN starting material.

<sup>d</sup>Lattice parameters are an average of the results for cubic C-BN compounds synthesized from both the microcrystalline C-BN starting materials and the mechanical mixtures of graphite-structured C and BN.

<sup>e</sup>Lattice parameter is derived from cubic C-BN synthesized from starting materials which are a mechanical mixture of graphite-structured C and BN.

equipped with a globar source and a triglycine sulfate detector and are reported with a resolution of  $4 \text{ cm}^{-1}$ .

For the high-pressure compression experiments, a mechanical mixture of the  $\text{C}_x(\text{BN})_{1-x}$  ( $x \sim 0.33$ ) composition, already converted to the high-pressure phase in a separate experiment, was loaded into a Mao-Bell-type diamond cell along with several ruby chips for pressure calibration. The sample was not converted *in situ* before x raying because the large volume change associated with the conversion from graphite-structured to cubic materials ( $\sim 15\%$  in volume) frequently results in damage to the diamond culets, which would prevent the experiment from reaching high pressures. The samples were compressed in a gasketed configuration using diamonds with  $200 \mu\text{m}$  culets and a 4:1 methanol:ethanol mixture to help maintain pseudohydrostatic conditions. X-ray-diffraction patterns were obtained at high-pressure by collimating  $\text{MoK}\alpha$  radiation generated by a Rigaku RU-200 rotating anode to an  $\sim 80 \mu\text{m}$  beam, and directing it through the axis of force of the diamond cell. High-pressure x-ray patterns were collected on film for four pressures between 15 and 100 GPa, with typical exposure times of 100–150 h.

## RESULTS

### Zero-pressure x-ray diffraction

The x-ray-diffraction patterns for the cubic C-BN solid solutions are listed in Table I with the high-pressure-temperature synthesis conditions given in Table II. The samples synthesized at high pressure and temperatures from the microcrystalline starting materials [ $\text{C}_{0.3}(\text{BN})_{0.7}$  and  $\text{C}_{0.6}(\text{BN})_{0.4}$ ] are primarily single-phase, with only one x-ray line which is not attributable to cubic C-BN: a weak line with a  $d$  spacing of  $3.345 \pm 0.005 \text{ \AA}$  appears in most of our zero-pressure C-BN x-ray films. As this is the strongest diffraction line (002) of C-BN in the graphite structure, the high-pressure reaction to the cubic phase is incomplete, resulting in the presence of a small amount of hexagonal, graphite C-BN as a contaminant probably along grain boundaries. Similarly, we note that x-ray patterns of cubic-BN, synthesized at General Electric, often have the (002) diffraction line of hexagonal boron nitride present.<sup>20</sup> There is no evidence of an exsolution between C (diamond) and cubic BN from any of our diffraction data using microcrystalline C-BN starting materials. Therefore, the composition of the high-pressure cubic phase is likely to be the same as that of the starting material.

Table I also illustrates the excellent agreement between the  $d$  spacings obtained from cubic C-BN synthesized from mechanical mixtures of graphite-structured C and BN and the microcrystalline starting materials for the  $\text{C}_{0.33}(\text{BN})_{0.66}$  [compare to  $\text{C}_{0.3}(\text{BN})_{0.7}$ ] and  $\text{C}_{0.6}(\text{BN})_{0.4}$  compositions. In addition to diffraction lines of cubic C-BN, the x-ray patterns of the three quenched mechanical mixtures include the (111) diffraction line of diamond and cubic BN. We attribute the presence of these lines to inhomogeneous regions in the starting material, i.e., where the graphitic-C and BN were not finely enough in-

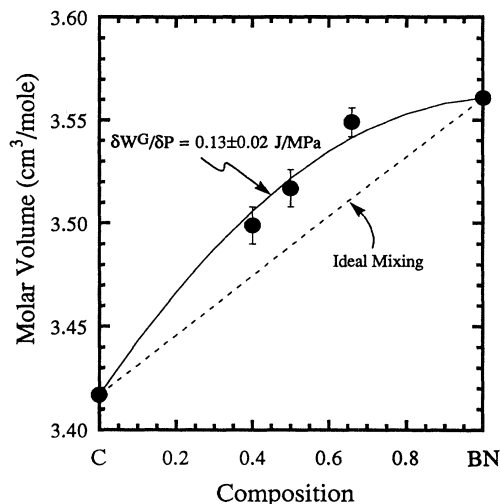


FIG. 1. The molar volume of cubic C-BN solid solutions. The straight, dashed line represents ideal mixing (Vegard's Law) between the endmember diamond and cubic BN, while the curved line is the fit to our solid solution data. We have determined the excess volume interaction (Margules) parameter,  $\delta W^G/\delta P$ , for this solid solution series to be  $0.13 \pm 0.02 \text{ J/MPa}$ . The datum of Badzian (1981) on the lattice parameter of a C-BN solid solution is not included because its composition is not independently known.

termixed. As with the samples synthesized from microcrystalline C-BN, these x-ray patterns also typically include a weak (002) reflection characteristic of graphite-structured compounds, implying that there is again some unreacted starting material in the quenched samples. We note that we do not observe any x-ray lines which could be indexed as superlattice lines of C-BN, as might be expected if the C-BN exhibited a high degree of ordering on different crystallographic sites. This is consistent with our assumption that C and BN form a complete solid-solution series.

Table II gives the lattice parameters obtained for each cubic C-BN solid solution, and the molar volumes are plotted in Fig. 1. As is evident from Fig. 1, the cubic C-BN compounds are nonideal solid solutions, with the incorporation of BN into the cubic diamond lattice resulting in expansion of the crystallographic unit cell relative to Vegard's law (ideal mixing).<sup>21</sup> Our results on the lattice parameters of cubic C-BN are difficult to compare directly with that of Badzian<sup>15</sup> because he estimated the composition of his sample material as  $\text{C}_{0.74}(\text{BN})_{0.26}$  based on the assumption of ideal mixing between diamond and borazon.

### Vibrational spectroscopy

The Raman and midinfrared absorption spectra of cubic  $\text{C}_{0.3}(\text{BN})_{0.7}$  (microcrystalline starting material) are shown in Fig. 2 with the frequencies listed in Table III. The infrared spectrum has a broad reststrahlen absorption peak between  $1000$  and  $1120 \text{ cm}^{-1}$  (we estimate that the samples are flakes  $1\text{--}2 \mu\text{m}$  thick dispersed in the KBr pellet). We do not observe any peaks due to multiphonon

TABLE III. Vibrational spectra for cubic C-BN solid solutions.

C (diamond) cm <sup>-1</sup>	C <sub>0.33</sub> (BN) <sub>0.67</sub> cm <sup>-1</sup>	BN (borazon) cm <sup>-1</sup>	Assignments
1331±2 (R) <sup>a</sup>			First-order phonon mode
	1323±2 (R)	1304±2 (R)	LO mode
	1053 <sup>b</sup> (R)	1056±2 (R)	TO mode
	1000–1120 (IR)	1000–1260 (IR) <sup>c</sup>	Reststrahlen band

<sup>a</sup>R indicates a Raman vibrational mode, IR indicates an infrared absorption mode.

<sup>b</sup>Estimated from the Lyddane-Sachs-Teller relation: see text.

<sup>c</sup>Reference 20.

absorption, perhaps because of the small amount of sample material (<0.1 mg) and the weakness of such vibrations. The reststrahlen peak of cubic C-BN is in a similar frequency range as the analogous band of cubic BN, which extends from  $\sim 1000\text{--}1260\text{ cm}^{-1}$  in the mid-infrared transmission spectrum.<sup>20</sup> Due to the width of the reststrahlen absorption for cubic C-BN, the value of the transverse-optic frequency ( $\nu_{\text{TO}}$ ) cannot be uniquely determined from this measurement. However, the presence of reststrahlen absorption confirms that cubic C-BN has more ionic character in its bonding than diamond, and that the transverse-optic mode is in a frequency range similar to that of cubic BN.

For the cubic C-BN quenched from high pressures, we measured only one Raman vibration, the longitudinal-optic mode ( $\nu_{\text{LO}}$ ) at  $1323\text{ cm}^{-1}$  [Fig. 2(b)]. For comparison, the Raman spectrum of diamond has only one first-order optic mode at  $1331\pm 2\text{ cm}^{-1}$ ,<sup>22</sup> whereas cubic BN has both a longitudinal- and a transverse-optic mode in its first-order Raman spectrum at 1304 and  $1056\text{ cm}^{-1}$ , respectively.<sup>23–25</sup>

We infer that the difference in these Raman spectra is due to the increase in ionic character of the B-N bond in the cubic-zinc-blende structure relative to the C-C bond in diamond. Therefore, because we observe the reststrahlen infrared absorption, we expect cubic C-BN to exhibit LO-TO splitting in its Raman spectrum in a manner similar to that of cubic BN. Our inability to measure the TO mode in the Raman spectrum of cubic C-BN may simply reflect the intrinsic weakness of the mode: the intensity ratio of LO to TO modes in zinc-blende structured semiconductors varies widely. For example, in ZnS (zinc blende), the LO mode measured in the Raman spectrum is about ten times as intense as the TO mode.<sup>26</sup> For our cubic C-BN samples, the signal-to-noise ratio of the Raman spectra is 4 to 1, implying that the TO mode need only be four times weaker than the LO mode to be unmeasurable in our experiments. The enhanced strength of the LO mode relative to the TO mode suggests that, for cubic C-BN, the polar contribution to the Raman scattering is more important than the deformation of the lattice.<sup>27</sup>

We can estimate the frequency of the TO mode in cubic C-BN from the value of the LO mode and an estimate of the dielectric constant using the Lyddane-Sachs-Teller relation:<sup>28</sup>  $\nu_{\text{LO}}^2 = (\epsilon_0/\epsilon_\infty)\nu_{\text{TO}}^2$  where  $\epsilon_0$  is the static dielectric constant and  $\epsilon_\infty$  is the high-frequency dielectric constant. Here,  $\nu_{\text{LO}} = 1323\text{ cm}^{-1}$  and we use the dielectric

constants of cubic BN to approximate those of cubic C-BN,  $\epsilon_0 = 7.1$  and  $\epsilon_\infty = 4.5$ .<sup>20</sup> Therefore, we estimate that the frequency of the TO mode of cubic C-BN is  $1053\text{ cm}^{-1}$ .

Although our compositional range is limited, we believe the  $\text{C}_x(\text{BN})_{1-x}$  system exhibits “one-mode” behavior of its optical phonons,<sup>29,30</sup> in contrast to most other III-V mixed crystals in the zinc-blende structure

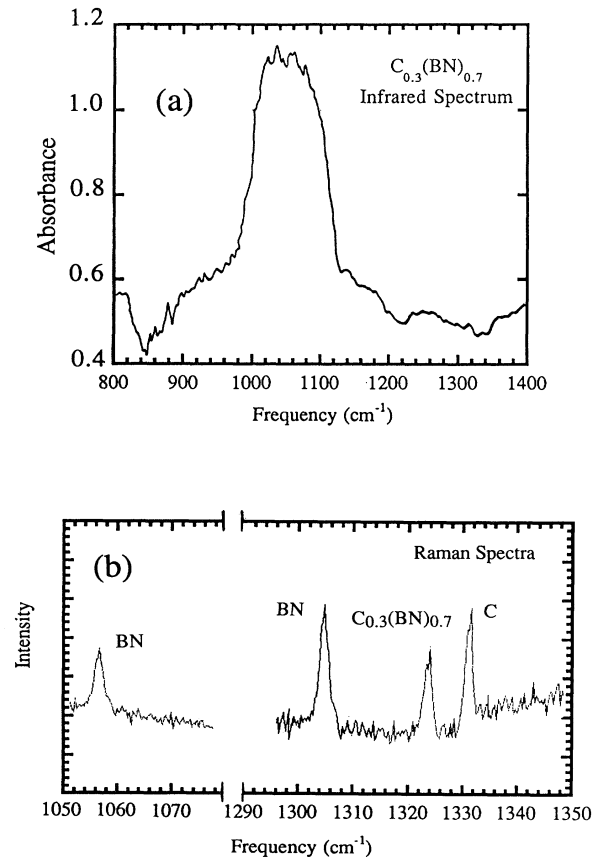


FIG. 2. (a) Infrared absorption spectrum of cubic  $\text{C}_{0.3}(\text{BN})_{0.7}$  (Table III lists the frequency range). (b) Comparison of the high-frequency Raman vibrations for diamond, cubic BN and cubic  $\text{C}_{0.3}(\text{BN})_{0.7}$  (see Table III). For diamond, the peak is a first-order optical mode with degenerate longitudinal and transverse components, whereas for cubic BN and cubic  $\text{C}_{0.3}(\text{BN})_{0.7}$ , it is the longitudinal-optic mode. The transverse-optic mode of cubic  $\text{C}_{0.3}(\text{BN})_{0.7}$  was too weak to measure.

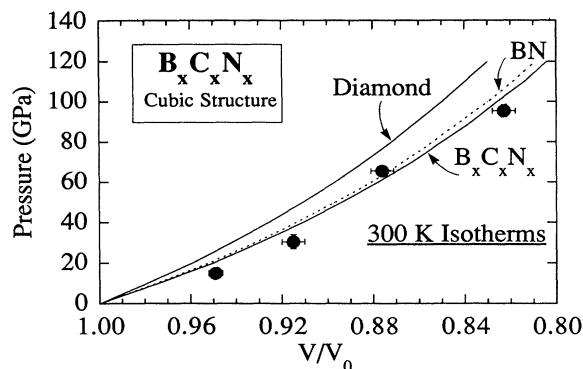


FIG. 3. Pressure-volume data (solid symbols) for cubic  $C_x(B_xN_x)$  measured using high-pressure x-ray diffraction at 300 K. The equation of state determined from a least-squares fit to this static-compression data is indicated. For comparison, the room-temperature isotherms for diamond and BN, calculated using an eulerian finite-strain equation of state formalism (Ref. 32) and the data in Refs. 2 and 3, is plotted.

(see Ref. 30 for a summary). That is, across the  $C_x(BN)_{1-x}$  solid solution, the first-order, degenerate Raman vibration of C (diamond) splits into LO and TO modes for  $x < 1$ , and for all the mixed crystal compositions, only one LO and one TO mode are observed. For comparison, most III-V mixed crystal compounds have two LO and two TO vibrational modes across the solid solution series, exhibiting “two-mode” behavior. Our observation for (metastable)  $C_x(BN)_{1-x}$  is similar to that of metastable  $Ge_x(GaAs)_{1-x}$ , also a mixed crystal containing a III-V semiconductor and a row IV element. Metastable  $Ge_x(GaAs)_{1-x}$  exhibits one-mode behavior<sup>31</sup> characterized by a shallow decrease of the LO mode of  $Ge_x(GaAs)_{1-x}$  between the Ge and GaAs endmember compositions, and a steep, nonlinear decrease of the TO frequency of  $Ge_x(GaAs)_{1-x}$  from Ge to GaAs.

#### High-pressure x-ray diffraction

The measured volumes and lattice parameters for cubic  $C_x(B_xN_x)$  ( $x \sim 0.33$ ) at high pressures are listed in Table IV and the isothermal equation of state is shown in Fig. 3 compared with the equations of state for diamond and BN. To determine the isothermal bulk modulus ( $K_{0T}$ ) for  $C_x(B_xN_x)$ , we have analyzed the data using an Eulerian finite-strain equation of state (Birch-Murnaghan equation: Ref. 32) which expresses pressure ( $P$ ) as an expansion in strain ( $f$ ):

$$P = 3K_{0T}f(1+2f)^{5/2}[1+af+bf^2 \dots],$$

TABLE IV. Static compression data for  $C_{0.33}(BN)_{0.67}$  starting material is a mechanical mixture of  $g$ -BN and  $g$ -C.

Pressure (GPa)	$V/V_0$	$hkl$	$a$ (Å)
$15.0 \pm 2.1$	$0.949 \pm 0.003$	111,220	$3.551 \pm 0.003$
$30.5 \pm 3.5$	$0.905 \pm 0.005$	111,220	$3.495 \pm 0.006$
$65.6 \pm 1.4$	$0.876 \pm 0.005$	111,220	$3.457 \pm 0.006$
$95.5 \pm 3.2$	$0.823 \pm 0.005$	111	$3.385 \pm 0.006$

TABLE V. Equation of state parameters for  $C_{0.33}(BN)_{0.67}$ .

$K_0$	$dK/dP$ ( $K'_0$ )	
$355 \pm 19^a$	4 (assumed)	Weighted average of $F^b$
$305 \pm 48$	4 (assumed)	Unweighted average of $F$
$228 \pm 71$	$9.4 \pm 3.5$	Linear $F$ vs $f$ fit, $K'_0$ unconstrained

<sup>a</sup>Preferred value: see text for discussion.

<sup>b</sup>See text for definition.

where  $f$  is the Eulerian strain parameter,  $[(V/V_0)^{-2/3} - 1]/2$ , and  $a$  and  $b$  are constants. In particular, the third-order coefficient ( $a$ ) is related to the pressure derivative of the bulk modulus ( $K'_0 = dK/dP$ ) as  $K'_0 = 2a/3 + 4$ . Usually, inclusion of the fourth-order ( $bf^2$ ) term is unnecessary. The choice of this equation of state reflects the empirical observation that it provides an excellent description of the compression of most solids.<sup>32-35</sup>

Using the method of Birch,<sup>32</sup> the data can be recast by formulating a normalized pressure,  $F$ , which equals  $P[3f(1+2f)^{5/2}]^{-1}$ . Therefore, if normalized pressure ( $F$ ) is plotted against strain ( $f$ ), the intercept  $F$  ( $f=0$ ) gives the bulk modulus ( $K_{0T}$ ) and the slope of the line is related to its pressure derivative ( $K'_0$ ). The data have been analyzed two ways. First,  $K'_0$  is assumed to be 4, which is equivalent to  $a=0$ : this value has been experimentally shown to reproduce compression data for a wide variety of substances. The bulk modulus is then an average of the values for  $F$ . Second, both  $K_{0T}$  and  $K'_0$  are fit from the data. The results for both analyses of the data are given in Table V. We consider the weighted fit with  $K'_0$  fixed at 4 to be the best value for the isothermal bulk modulus, as  $K'_0 = 9.38(\pm 2.5)$  is considered unusually large for most solids,<sup>34</sup> and is completely incompatible

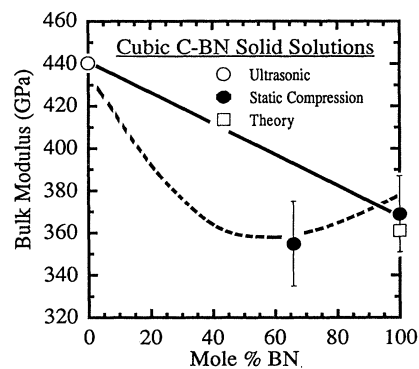


FIG. 4. Comparison of the isothermal bulk moduli for diamond, cubic BN and cubic  $C_x(B_xN_x)$ . The bulk modulus of cubic C-BN is smaller than expected for ideal mixing of diamond and cubic BN (solid line). The dashed line is a prediction of the bulk modulus based on the measured nonideal expansion of the unit-cell volume, and a linear relationship between crystal density ( $\rho$ ) and bulk sound velocity  $[(K_s/\rho)^{1/2}]$ . The bulk modulus of diamond shown here (open circle) is derived from the ultrasonic measurements of McSkimin and Andreatch (Ref. 2) and the static compression (closed circle) and theoretical (open square) results for cubic BN are from Knittle *et al.* (Ref. 3).

with the values of  $K'_0$  for diamond and cubic-BN<sup>3</sup>. In addition, for extremely incompressible solids such as cubic C-BN, data at very high pressures are necessary to accurately determine  $K'_0$ ; therefore, our fit which weights  $F$  by its error (as  $1/\sigma^2$ ) is likely to provide the best estimate of  $K_{0T}$ .<sup>36</sup>

The isothermal bulk modulus of cubic  $C_x(B_xN_x)$  is compared with the values for diamond and cubic BN in Fig. 4. As would be expected from the nonideality in lattice parameter, the bulk modulus of  $C_x(B_xN_x)$  is smaller than predicted based on its stoichiometry. However, this material still has one of the largest bulk moduli, 355 ( $\pm 19$ ) GPa, known for any solid.

### DISCUSSION

The nonideality of the molar volumes in the cubic C-BN system can be described with a standard mixing model where the excess volume term  $\Delta V^{xs} = X_1 X_2 (\delta W^G / \delta P)$ .<sup>37,38</sup> Here,  $X_1$  and  $X_2$  are the mole fractions of cubic C and BN and  $W^G$  is the interaction (or Margules) parameter. When expressed as a function of the mole fraction of carbon only ( $X_c$ ), this equation becomes a polynomial:  $\Delta V^{xs} = X_c (1 - X_c) (\delta W^G / \delta P)$ . Therefore, from the zero-pressure x-ray-diffraction data for cubic C-BN compounds, the deviation from ideality for the volume can be determined as a function of mole fraction of diamond and hence  $\delta W^G / \delta P$  calculated at 1 bar. We find that  $\delta W^G / \delta P = 0.13 \pm 0.02$  J/MPa and the maximum deviation from ideality is  $\sim 1\%$  in volume. Figure 1 illustrates the fit of the nonideal volume model to the data. With our model we can reinterpret the datum of Badzian (Ref. 15) with its lattice parameter of  $3.582 \pm 0.002$  Å to correspond to a stoichiometry of  $C_{0.85}(BN)_{0.15}$ .

The result for the measurement of the bulk modulus of the  $C_x(B_xN_x)$  solid solution is consistent with expansion of the lattice parameters and molar volume away from ideality in that the bulk modulus is smaller ( $\sim 10\%$ ) than expected for ideal mixing between cubic BN and C. We note that the measured bulk modulus is consistent with scaling arguments for the relationship between the nearest-neighbor distance and bulk modulus in diamond and zinc-blende structures.<sup>39</sup> For  $C_x(B_xN_x)$ , the nearest-neighbor distance is  $1.564 \pm 0.002$  Å which, according to Cohen's relation  $K_{0T} = (1971 - 220\lambda)d^{-3.5}$  (here we assume that  $\lambda = 1$  which is appropriate for a III-V compound), yields a bulk modulus estimate of 368 GPa consistent with the measured value of 355 ( $\pm 19$ ) GPa.

In addition, from the model of the nonideal volumes, and hence densities of  $C_x(BN)_{1-x}$  solid solutions, we can predict the deviation of the bulk modulus from ideality as a function of composition. We use the observation that for solids with the same structure, the relationship between density and bulk sound velocity,  $(K_s/\rho)^{1/2}$  where  $K_s$  is the adiabatic bulk modulus and  $\rho$  is the density, is empirically found to be linear.<sup>40</sup> Therefore, using the density and measured bulk modulus for diamond, cubic BN and  $C_{0.3}(BN)_{0.7}$ , we find that  $(K_s/\rho)^{1/2} = 19.5(\pm 3)\rho - 57.5(\pm 12)$ . So, from the densities of the

$C_x(BN)_{1-x}$  compositions derived from Fig. 1, the bulk modulus can be predicted across the C-BN solid solution as illustrated in Fig. 4.

Comparison of the vibrational spectra of diamond, cubic BN and cubic- $C_{0.3}(BN)_{0.7}$ , allows us to investigate the nature of the bonding in cubic C-BN. The high-frequency Raman mode in diamond, the zero-center optical phonon, is 21% higher than the frequency of the comparable TO mode in cubic BN. Most of the decrease in frequency can be attributed to the increased ionicity of the B-N bond and not to the effects of the increased mass or longer bond lengths in B-N relative to C-C.<sup>24,25</sup> To demonstrate this, we use the familiar expression that the observed frequency of vibration  $\nu$  is proportional to  $(k/\mu)^{1/2}$ , where  $k$  is the force constant of the bond and  $\mu$  is the reduced mass of the two components of a harmonic oscillator [ $\mu = (m_1 m_2) / (m_1 + m_2)$ ], to estimate the reduction in vibrational frequency between diamond and cubic BN due to mass alone. For the C-C bond in diamond,  $\mu_{C-C} = 6.0055$  and, for the B-N bond in cubic BN,  $\mu_{B-N} = 6.102$ . If the force constants are assumed to be approximately equal between the two solids, then only about 1% of the reduction in frequency can be attributed to the increase in mass of B-N versus C-C.

Similarly, we can estimate the effect of longer bond lengths in cubic BN relative to diamond on lowering the vibrational frequency. Again, simple scaling arguments can be used to estimate the magnitude of this reduction. The frequency  $\nu$  is approximately proportional to  $d^{-3/2}$  where  $d$  is the nearest-neighbor distance.<sup>41</sup> For diamond,  $d = 1.545 \pm 0.002$  Å, and for cubic BN,  $d = 1.566 \pm 0.002$  Å; therefore, only a 2% further reduction in vibrational frequency might be expected from the increase in bond length. Therefore, we conclude that the difference between the first-order vibrational frequency in diamond and the TO mode of cubic BN reflects the greater bond strength in diamond.

The case for cubic  $C_{0.3}(BN)_{0.7}$  is interesting in that all of the measured increase in vibrational frequency between cubic BN and cubic  $C_{0.3}(BN)_{0.7}$  can be explained by the net decrease in mass when C-C pairs are substituted for B-N in the zinc-blende structure, and the decrease in nearest-neighbor distance of cubic  $C_{0.3}(BN)_{0.7}$  relative to cubic BN. If we calculate the reduced mass for C-N and C-B pairs and average them, then the predicted increase in vibrational frequency, assuming that the force constant is the same as that for cubic BN, is  $\sim 1\%$ . An additional increase in frequency of 0.2% is expected from the decrease in nearest-neighbor distance between cubic  $C_{0.3}(BN)_{0.7}$  and cubic BN. From this analysis, we predict  $\nu_0 = 1320$  cm<sup>-1</sup> for cubic  $C_{0.3}(BN)_{0.7}$ , in good agreement with what is observed. Therefore, bonding in cubic C-BN has a substantial amount of ionic character, similar to cubic BN and unlike diamond where the bonding is purely covalent.

We can use the expression of Pauling<sup>42</sup> to estimate the ionicity of bonds in the cubic C-BN structure: Fractional ionicity  $= 1 - \exp[-0.25(\chi_a - \chi_b)^2]$ , where  $\chi_a$  and  $\chi_b$  are the electronegativities of the atoms participating in the bond. For the B-N bond, the estimated fractional

ionicity is 0.22, implying that 22% of the bonding is due to electrostatic forces rather than covalency. For a C-B bond,  $\chi_C=2.55$  and  $\chi_B=2.04$  which implies a 6% ionic contribution to the bond strength. Similarly, for the C-N bond,  $\chi_N=3.04$  and the C-N bond is about 6% ionic. Ionicity of 6% is quite low. For instance, calculations on the effect of boron on the charge density of carbon in  $BC_3$  show that the electron density of carbon bonds are relatively unperturbed by the addition of boron.<sup>43</sup> However, the x-ray diffraction of the present samples shows that they are disordered. Therefore, the presence of any B-N bonds in cubic C-BN will contribute to the overall ionic character of the bonding in the crystal. We speculate that, if cubic C-BN were an ordered structure with every B and N atom bonded to a carbon, then the structure would be significantly more covalent.

### CONCLUSIONS

Cubic, zinc-blende-structured  $C_x(BN)_{1-x}$  solid solutions can be synthesized at pressures greater than 30 GPa and temperatures above 1500 K. Measurements of the lattice parameters of  $C_x(BN)_{1-x}$  samples quenched to ambient pressure show that the solid solution series is nonideal, with molar volumes up to 1% larger than expected based on ideal mixing between C (diamond) and cubic-BN. We also find that the bulk modulus of

$C_{0.3}(BN)_{0.7}$  is 355 ( $\pm 19$ ) GPa, smaller than would be predicted for an ideal solid solution of C and cubic BN, but consistent with the expanded unit-cell volumes. In addition to the measurement of the mechanical properties of  $C_x(BN)_{1-x}$  solid solutions, we have investigated the bonding in  $C_{0.3}(BN)_{0.7}$  by measuring the infrared and Raman spectra. We find that the vibrational spectra of  $C_{0.3}(BN)_{0.7}$  exhibit LO-TO splitting of the phonon modes, which indicates that there is an ionic contribution to the bonding in these solid solutions. Therefore,  $C_x(BN)_{1-x}$  solid solutions are considerably more similar to cubic BN than to diamond in their bonding properties.

### ACKNOWLEDGMENTS

We thank M. Kruger for running the infrared spectrum. N. Bartlett, Q. Williams, and M. Kruger provided helpful discussion. This work was supported by the A. P. Sloan Foundation (E.K.), the W. M. Keck Foundation (UCSC), the Donors of the Petroleum Research Fund, Grant No. 21622AC7-C (R.B.K.), the National Science Foundation Grant No. DMR-9120269 (M.L.C.), the Office of Energy Research, Office of Basic Energy Sciences, Materials Sciences Division of the U.S. Department of Energy under Contract No. DE-AC03-76SF00098 (M.L.C. and R.J.), and UCSC Institute of Tectonics (Mineral Physics Lab) Contribution No. 176.

\* Author to whom correspondence should be addressed.

<sup>1</sup>R. C. De Vries, *Cubic Boron Nitride: A Handbook of Properties*, GE Report No. 72CRD178, 1972.

<sup>2</sup>H. J. McSkimin and P. J. Andreatch, *J. Appl. Phys.* **43**, 2944 (1972).

<sup>3</sup>E. Knittle, R. M. Wentzcovitch, R. Jeanloz, and M. L. Cohen, *Nature (London)* **337**, 349 (1989).

<sup>4</sup>T. Akashi, A. Sawaoka, and S. Saito, *J. Am. Ceram. Soc.* **61**, 245 (1978).

<sup>5</sup>F. P. Bundy and R. H. Wentorf, *J. Chem. Phys.* **38**, 1144 (1963).

<sup>6</sup>N. L. Coleburn and J. W. Forbes, *J. Chem. Phys.* **48**, 555 (1968).

<sup>7</sup>F. R. Corrigan and F. P. Bundy, *J. Chem. Phys.* **63**, 3812 (1975).

<sup>8</sup>P. S. DiCarli, *Bull. Am. Phys. Soc.* **12**, 1127 (1967).

<sup>9</sup>W. H. Gust and D. A. Young, *Phys. Rev. B* **15**, 5012 (1977).

<sup>10</sup>A. Onodera, H. Miyazaki, and N. Fujimoto, *J. Chem. Phys.* **74**, 5814 (1981).

<sup>11</sup>H. Sumiya, T. Iseki, and A. Onodera, *Mater. Res. Bull.* **18**, 1203 (1983).

<sup>12</sup>R. H. Wentorf, *J. Chem. Phys.* **26**, 956 (1957).

<sup>13</sup>R. H. Wentorf, *J. Chem. Phys.* **34**, 809 (1961).

<sup>14</sup>S. Yamaoka, O. Shimomura, M. Akaishi, H. Kanda, T. Nagashime, O. Fukunaga, and S. Akimoto, *Physica B* **139-140B**, 668 (1986).

<sup>15</sup>A. R. Badzian, *Mater. Res. Bull.* **16**, 1385 (1981).

<sup>16</sup>R. B. Kaner, J. Kouvetakis, C. E. Warble, M. L. Sattler, and N. Bartlett, *Mater. Res. Bull.* **22**, 399 (1987).

<sup>17</sup>H. K. Mao, P. M. Bell, J. W. Shaner, and D. J. Steinberg, *J. Appl. Phys.* **49**, 3276 (1978).

<sup>18</sup>D. Heinz and R. Jeanloz, in *High Pressure Research in Mineral Physics*, edited by M. H. Manghni and Y. Syono, (American Geophysical Union, Washington, DC, 1987), p. 113.

<sup>19</sup>Q. Williams, E. Knittle, and R. Jeanloz, *J. Geophys. Res.* **96**, 2171 (1991).

<sup>20</sup>P. J. Gielisse, S. S. Mitra, J. N. Plendl, R. D. Griffis, L. C. Mansur, R. Marshall, and E. A. Pascoe, *Phys. Rev.* **155**, 1039 (1967).

<sup>21</sup>L. Vegard, *Z. Phys.* **5**, 17 (1921).

<sup>22</sup>S. A. Solin, and A. K. Ramdas, *Phys. Rev. B* **1**, 1687 (1970).

<sup>23</sup>O. Brafman, G. Lengyel, S. S. Mitra, P. J. Gielisse, J. N. Plendl, and L. C. Mansur, *Solid State Commun.* **6**, 523 (1968).

<sup>24</sup>I. V. Aleksandrov, A. F. Goncharov, S. M. Stishov, and E. V. Yakovenko, *JETP Lett.* **50**, 127 (1989).

<sup>25</sup>J. A. Sanjurjo, E. Lopez-Cruz, P. Vogl, and M. Cardona, *Phys. Rev. B* **28**, 4579 (1983).

<sup>26</sup>L. Couture-Mathieu and J. P. Mathieu, *C. R. Acad. Sci.* **236**, 371 (1953).

<sup>27</sup>R. Loudon, *Adv. Phys.* **13**, 423 (1964).

<sup>28</sup>R. H. Lyddane, R. G. Sachs, and E. Teller, *Phys. Rev.* **59**, 673 (1941).

<sup>29</sup>A. S. Barker and A. J. Sievers, *Rev. Mod. Phys.* **47**, Suppl. 2, S1 (1975).

<sup>30</sup>G. P. Srivastava, *The Physics of Phonons* (IOP, New York, 1990), p. 294.

<sup>31</sup>S. A. Barnett, M. A. Ray, A. Lastras, B. Kramer, J. E. Greene, P. M. Raccach, and L. L. Abels, *Electron. Lett.* **18**, 891 (1982).

<sup>32</sup>F. Birch, *J. Geophys. Res.* **83**, 1257 (1978).

- <sup>33</sup>F. Birch, *J. Geophys. Res.* **57**, 227 (1952).
- <sup>34</sup>E. Knittle, in *Handbook of Physical Constants*, edited by T. J. Ahrens (American Geophysical Union Press, Washington, DC, in press).
- <sup>35</sup>R. Jeanloz, *J. Geophys. Res.* **94**, 5873 (1989).
- <sup>36</sup>P. M. Bell, H. K. Mao, and J. A. Xu, in *High Pressure Research in Mineral Physics*, edited by M. H. Manghnani and Y. Syono (American Geophysical Union, Washington, DC, 1987), p. 447.
- <sup>37</sup>E. A. Guggenheim, *Trans. Faraday Soc.* **33**, 151 (1937).
- <sup>38</sup>H. K. Hardy, *Acta Metall.* **1**, 202 (1953).
- <sup>39</sup>M. L. Cohen, *Phys. Rev. B* **32**, 7988 (1985).
- <sup>40</sup>T. J. Shankland, *J. Geophys. Res.* **77**, 3750 (1972).
- <sup>41</sup>S. S. Batsanov, and S. S. Derbeneva, *J. Struct. Chem.* **10**, 510 (1969).
- <sup>42</sup>L. Pauling, *The Nature of the Chemical Bond* (Cornell University Press, Ithaca, 1960), p. 98.
- <sup>43</sup>D. Tomanek, R. M. Wentzcovitch, K. J. Chang, and M. L. Cohen, *Phys. Rev. B* **37**, 3134 (1988).